3nd International Symposium on Friction Stir Welding, Kobe, Japan, 27 and 28 September 2001, TWI (UK)

Investigations on Residual Stresses in Friction Stir Welds

C. Dalle Donne, Institute of Materials Research, German Aerospace Center, D-51170 Cologne Germany

E. Lima, J. Wegener, A. Pyzalla, Hahn-Meitner-Institut Berlin, D-14109 Berlin, Germany

T. Buslaps, European Synchrotron Radiation Facility ESRF, F- 38043 Grenoble, France

Introduction

Because of the low temperature level compared to fusion welding techniques, it is generally believed that residual stresses are low in friction stir welds. However, the very rigid clamping arrangement exerts a much higher restraint on the deformation of the welded plates than the more compliant clamps used for fixing the parts during conventional welding processes. These restraints impede the contraction due to cooling of the weld nugget and heat affected zone in longitudinal as well as in transverse direction, introducing transverse and longitudinal residual stresses, Figure 1.

The residual stress distribution shown in Figure 1 is a very simple one typically encountered in steel weldments [1]. So far residual stress measurements have been reported for friction stir welded 7xxx alloys in [2, 3]. Djapic Oosterkamp et al. [2] investigated longitudinal residual stresses in 80 x 60 x 6 mm^3 of extruded 7108-T79 aluminium alloy. The peak values of around 140 MPa (57% of weld material yield strength or 47 % of parent material yield strength) were found in the on advancing side of the weld near the top surface of the plate. Jata et al. [3] measured residual stresses in 5.1 mm thick and 24.5 mm wide single edge notched specimens of welded 7050-T7451. They showed that in the rather small specimens the longitudinal residual stresses were higher than the transverse stresses. Peak values of around 100 MPa (34% of weld material yield strength or 20 % parent material yield strength)

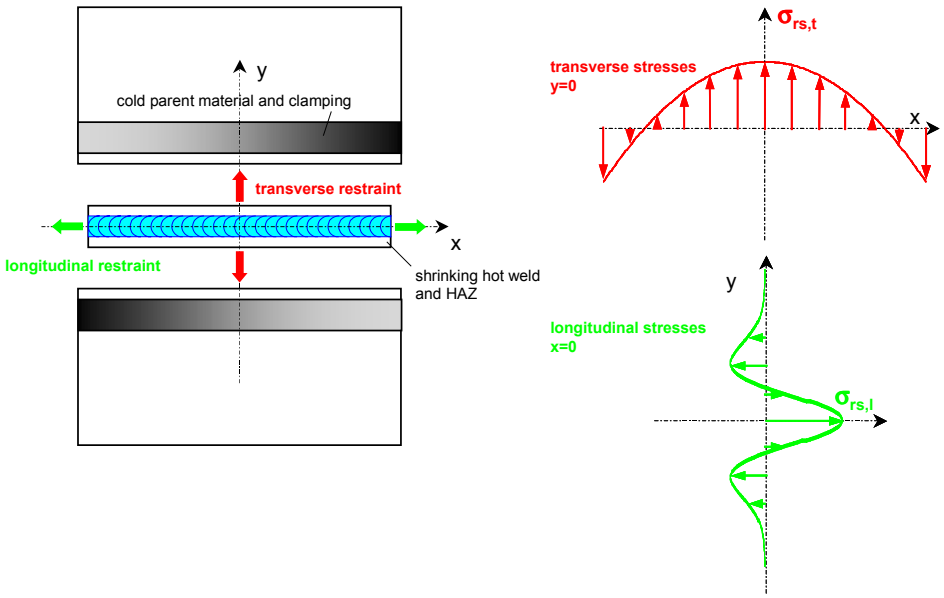

Figure 1: Schematic of the restraint exerted by the cooler parts of the plates and the clamping on the HAZ and the weld. These restraints cause residual stresses in welding direction (longitudinal) and perpendicular to it (transverse).

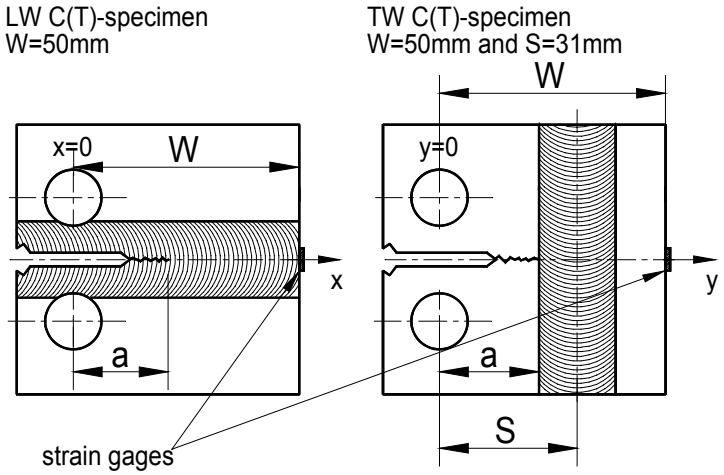

Figure 2: Welded specimen configurations.

were found near root or back surface of the weld.

Wang et al. [17] studied residual stresses in 200 x 200 x 6 mm^3 large coupons of 6061-T6 by neutron diffraction. They found an increase of longitudinal residual stresses with increasing weld speed and maximum tensile values of 200 MPa. This corresponds to 73 % of the parent material yield strength.

Cut compliance measurements on welded 50 mm wide compact tension specimens (C(T)) of 4 mm thick 2024-T3 and 6013-T6 were carried out by one of the authors [4, 5]. The residual stresses were however presented in terms of a stress intensity factor, which was used for the calculation of the true load ratio or mean stress level during fatigue crack propagation tests. On the basis of an effective stress intensity factor approach it was shown that the differences between parent material and FSW fatigue crack propagation curves were mainly caused by the residual stresses in the welded specimens. In other words, the real resistance against fatigue crack growth of the friction stir welded specimens was equal to the parent material resistance. Therefore it was possible to predict the constant amplitude da/dN-ΔK curves of the welded specimens on the basis of parent material data and the residual distribution normal to the crack plane .

In the first part of the paper cut compliance data of the welded C(T) specimens is shortly reviewed and the residual stress distribution is approximately calculated using the inverse weight function method.

In the second part of the paper the residual stress state in welded plates of 4mm 6013-T4 is discussed more in detail. The residual stress state in the whole joints is characterised using X-rays for the determination of the residual stresses at the top and the root surface as well as by using high energy synchrotron radiation and neutrons for the measurement of the residual stresses in the bulk of the joints. The effects of welding parameters (rotational speed, transverse speed, tool size) on the residual stresses are discussed.

Residual Stress Distributions in Compact Tension Specimens

Materials, FSW and Specimens

Two types of 4 mm thick aluminum alloy sheets, 2024-T3 and 6013-T6, were welded on conventional milling machines at DLR and EADS Corporate Research Center on the basis of the TWI patent. The welding direction was always in rolling direction. The ultimate tensile strength values of the joints were in the range of 90 % (2024-T3) and 80 % (6013 welded in T4 and aged to T6 after welding) of the parent material's ultimate strength. Further details

such as process parameters, microstructures, hardness distributions and strength values are found in [5-7].

The "longitudinal weld" LW specimens had cracks in the center of the weld propagating parallel to the welding direction, Figure 2. In [4, 5] differences and changes in crack propagation rate da/dN of the LW-specimens were attributed to transverse residual stresses acting in the direction perpendicular to the weld and crack propagation direction. In the "transverse weld" TW specimens the crack approached the weld perpendicularly, Figure 2. In these specimens longitudinal residual stresses (parallel to the weld) were responsible for pronounced effects on da/dN at constant ΔK [4].

Residual stress intensity factor measurement

The stress intensity factor due to residual stresses K_{rs} was determined directly with the so called "cut compliance method" [8, 9]. The method is based on the crack compliance method: a narrow saw cut is introduced progressively in the potential crack plane of the considered specimen or component and the resulting strain change is measured by a strain gauge. The desired stress intensity factor is proportional to the slope of the measured strain ε plotted as a function of the depth of the cut (i. e. crack length a):

$$K_{rs} = \frac{E'}{Z(a)} \frac{d\varepsilon}{da} \qquad Z(a) = -\frac{2.532}{(W-a)^{1.5}} \left(1 - e^{-6.694 \frac{a}{W}}\right) \qquad (1)$$

The proportionality factor or influence function Z(a) is a unique function, that depends only on the cut depth, the geometry of the specimen or component and the strain measurement location. In this investigation a strain gage was glued on the C(T) specimen at the location indicated in Figure 2.

The cut compliance method delivers the residual stress as a stress intensity factor, suitable for direct use in fracture mechanical assessments. The elastic re-distribution of residual stresses with increasing crack or slit length is already included in the K_{rs} versus a solution. Further details may be found in [9].

The residual stresses can be determined from the stress intensity factor by using a weight function solution:

$$K_{rs,t}(a) = \int_{a_0}^{a} h(x,a)\, \sigma_{rs,t}(x)\, dx \qquad K_{rs,l}(a) = \int_{a_0}^{a} h(y,a)\, \sigma_{rs,l}(y)\, dy \qquad (2)$$

where h is the weight function, which is available for a wide variety of geometries [10]. Equation 2 can be solved for the residual stresses by approximating the stress distribution with n constant values, σ_j, within each of n intervals a_n-a_{n-1}. This gives the discrete form of eqn. (2), which can be solved for the residual stresses $\sigma_{rs,t,j}$ and $\sigma_{rs,t,j}$ [11]:

$$K_{rs,t}(a_i) = \sum_{j=1}^{i} \sigma_{rs,t,j} \int_{a_{j-1}}^{a_j} h(x,a_i)\, dx \qquad K_{rs,l}(a) = \sum_{j=1}^{i} \sigma_{rs,l,j} \int_{a_{j-1}}^{a_j} h(y,a_i)\, dy \qquad (3)$$

Here the weight function for a single edge notched specimen was used [12]. The accuracy of the approach was checked by re-calculating the residual stress profile given in [13] on the basis of the published finite element data. Virtually the same residual stress distribution as the one given in [13] was obtained.

Figure 3 shows the distribution of K_{rs} measured by introducing an 0.3 mm wide fret saw cut in the ligament of the welded C(T) specimens. Mean values of at least 2 cutting test were used for one curve. The negative stress intensity factors of Figure 3 are related to compressive

residual stresses ahead of the crack. This is shown in Figure 4, where the approximate initial residual stress distribution was calculated numerically with eqn. (3).

Obviously only the crack opening residual stresses are evaluated with this method. In the longitudinal weld specimens, the transverse residual stresses re-arrange after a crack growth increment in such way that compressive stresses are maintained at the crack tip. With increasing crack length the magnitude of the compressive residual stresses decreases and finally only small amounts of tensile stresses are active at the tips of long cracks. This can be proven by calculating the residual stress distribution after some amounts of crack growth with Schindler's inverse weight function method (not shown here).

Cutting of TW-specimens out of the 6013-T6 plates resulted also in compressive residual stresses ahead of the crack, Figure 4 right side. The longitudinal residual stresses are however higher in magnitude than transverse stresses and two peaks are reached in the heat affected zones of the weld.

The absolute compressive peak value of the residual stress just ahead of the notch strongly

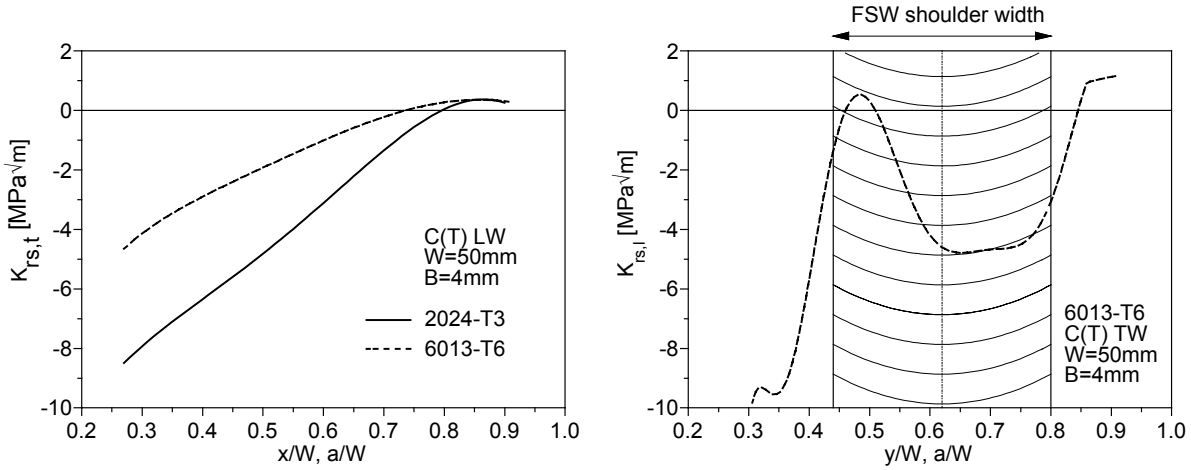

Figure 3: Distribution of the stress intensity factor due to residual stresses in the ligament of the C(T) specimens (left: longitudinal weld specimen, right: transverse weld specimen).

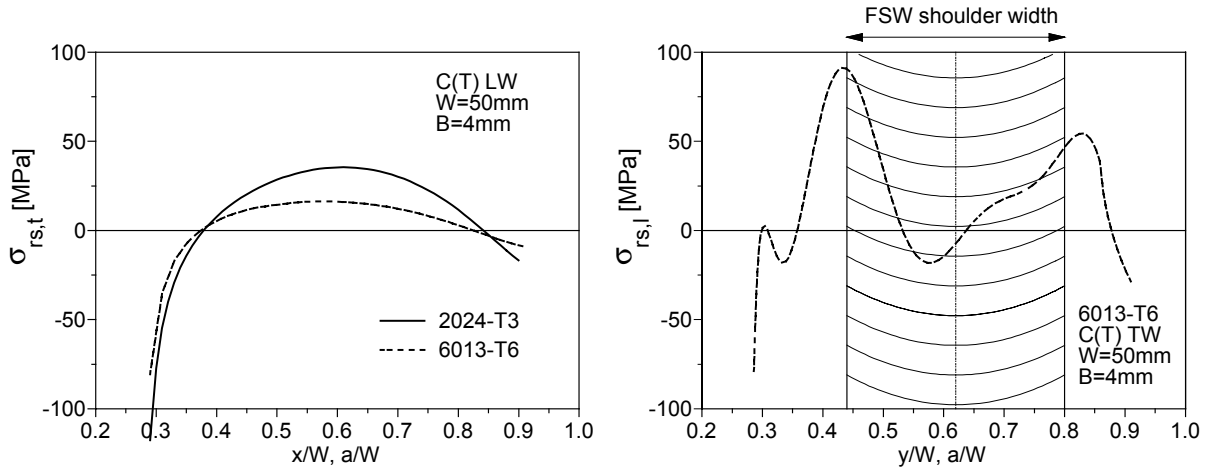

Figure 4: Approximate distribution of the transverse residual stresses in the ligament of the LW specimen (left) and of the longitudinal residual stresses in the ligament of the TW specimen.

depends from the result of the first cut and can therefore not be considered as a reliable value [13]. The compressive transverse stresses were approximately in the order of – 80 MPa for 6013-T6 (27 % of weld material yield strength or 23 % parent material yield strength) and of less than – 100 MPa for 2024-T3 (over 35 % of weld material yield strength or 30 % parent material yield strength). The highest tensile residual stresses were reached on the advancing side edge of the tool shoulder foot print in the 6013-T6 TW specimen (longitudinal residual stresses) with 91 MPa (31 % of weld material yield strength or 26 % parent material yield strength).

Experimental Residual Stress Analyses by Diffraction Methods

Material and FSW

A different batch of 6013 material was used in this investigation. All welds were performed in rolling direction and T4 heat treatment condition. In the T4 condition the parent material had a yield strength of 224 MPa and an ultimate strength of 320 MPa. No additional heat treatment was carried out after welding. The welding parameters are summarized in Table 1 together with the data of the welds used for the cut compliance investigation. The yield strength of the joints varied between 170 to 180 MPa whereas ultimate strength levels varied between 270 and 290 MPa. Generally the strength increased with increasing weld speed. The strength tests were carried out within two weeks after welding. It turned out later, that room temperature aging took place over a period of over one month, so that 20 MPa higher yield and ultimate strength may be expected in the specimens used for residual stress measurements. The approximate in plane dimensions of the samples are also given in Table 1 (weld seam in shorter direction).

Table 1: Welding parameters and in-plane sample sizes.

material	rotation [min^{-1}]	weld speed [mm/min]	Shoulder diameter [mm]	pin diameter [mm]	sample size [mm]
6013-T4	1000	300	22	6	30 x 80
6013-T4	1500	300	22	6	30 x 80
6013-T4	1670	500	15	4	60 x 80
6013-T4	2500	1000	15	4	60 x 80
6013-T6 [1]	1400	400	18	6	60 x 62 (CT)

[1)] cut compliance tests, different batch of 6013 welded in T4 and aged to T6 after welding
gage length 50 mm

Experimental details

In contrast to the method outlined before, non-destructive techniques based on residual lattice strains determined with diffraction methods are used in this section. From the residual lattice strains the residual stresses can be calculated using Hooke's law.

To analyze the residual stress distribution throughout the weld, different radiations have to be used. Conventional X-rays have a penetration depth of several µm up to some 10µm in aluminium. Thus, using conventional X-rays, the residual stresses at the front and the bottom side of the weld can be determined. The resolution in the in-plane direction is approximately 2 mm.

In order to evaluate through-thickness residual stresses the use of neutrons or high energy synchrotron radiation is necessary. Neutrons have a penetration depth of several millimetres in most materials. In case of aluminium alloys the penetration depth of neutrons reaches some 10 millimetres. The available neutron flux extends the gauge volume to the order of some cubic millimetres. Therefore, the residual stress values obtained by neutron diffraction average across larger areas of the weld and in particular across the sheet and weld thickness.

In case of high energy synchrotron the flux and the parallelism of the radiation are significantly higher than in case of neutrons. Due to the low absorption at high energy values in case of light weight alloys penetration depths comparable to those of neutrons can be reached. A new technique using white high energy synchrotron radiation permits the use of gauge volumes as small as 60 µm x 60 µm x 500 µm [14,15]. Thus, residual stress analyses with a very high local resolution are possible in the friction stir weld.

For determining the residual stresses in the near surface area on the top and the bottom side of the weld conventional X-rays were employed in a laboratory at the HMI Berlin. By using Co-Ka and Cu-Ka radiation slightly different penetration depths were achieved. The measurements were performed on a Ψ – diffractometer using the $\sin^2\psi$ –method.

Neutron diffraction measurements were carried out at the dedicated residual stress diffractometer E3 at the BER II reactor. Monochromatic radiation with a wavelength of ~1,37 nm was used. The strains were obtained from the 2θ - shift of the {311} reflection. The position of the gauge volume of 2 mm x 2 mm x 2 mm was defined by a slit in the incoming neutron beam and a second slit in the diffracted neutron beam.

Residual stress analyses using high energy synchrotron radiation were performed at the beamline ID15a of the European Synchrotron Radiation Facility (ESRF) in Grenoble, France. An energy dispersion arrangement with an incoming white beam was used. A germanium semiconductor detector was positioned at a diffraction angle 2θ = 10°. The gauge volume was

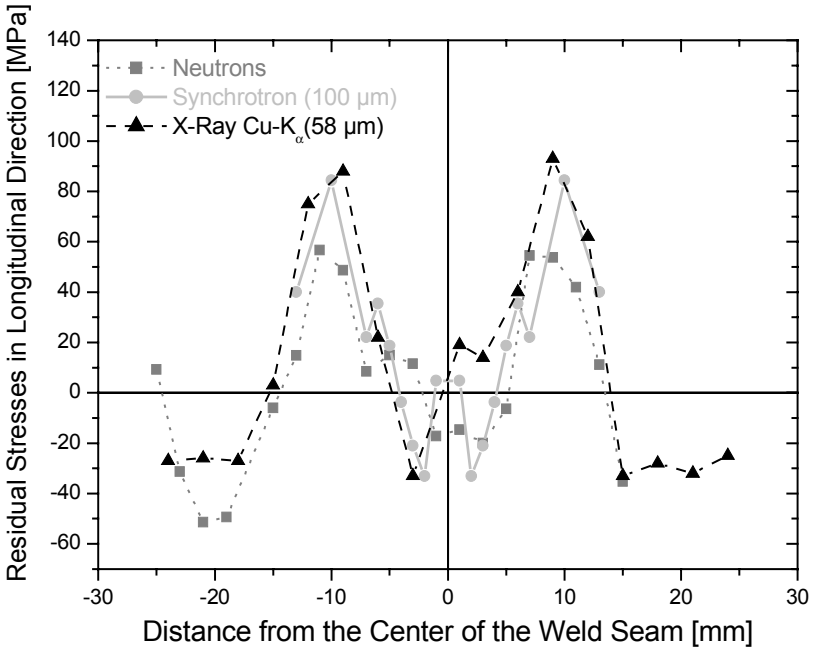

Figure 5: Residual stresses distribution along the weld of a friction stir welded 6013-T4 sheet determined with different measurement methods. Sample welding parameters: tool rotational speed: 2500 min^{-1}; welding speed: 1000 mm s^{-1}; tool shoulder diameter: 15 mm.

defined by 100 µm wide slits in the incoming and 80 µm wide slits in the diffracted beam to a size of 80 µm x 100 µm x 920 µm. The d_0 value in different positions across the weld was calculated from stress equilibrium conditions.

Results

The results of the residual stress analyses reveal that the residual stress distribution is inhomogeneous in the longitudinal, in the transverse direction of the weld as well as across the thickness of the weld.

In longitudinal and in transverse direction of the weld, in all specimen examined here, diffraction methods yield an "M" like stress distribution across the weld, which is in good agreement with the residual stress distribution obtained from the cut compliance measurements described in the previous sections of this paper. A direct comparison with the cut compliance results makes no sense, because of the different material batch, heat treatment and sample size.

The maximum values of the tensile residual stresses are located in the heat affected zone. From these maximum values the tensile residual stresses decrease and the parent material adjacent to the heat affected zone as well as the weld seam contain small compressive residual stresses. With increasing distance to the weld the residual stresses then gradually change into the initial stress state of the sheet material.

In all samples investigated, independent on the pin diameter, the welding speed and rotational speed of the tool, the maximum of the residual stresses were higher in longitudinal direction than in transverse direction. Therefore only the residual stress distributions in longitudinal direction $\sigma_{rs,l}$ of the welds is presented in Figures 5 to 7.

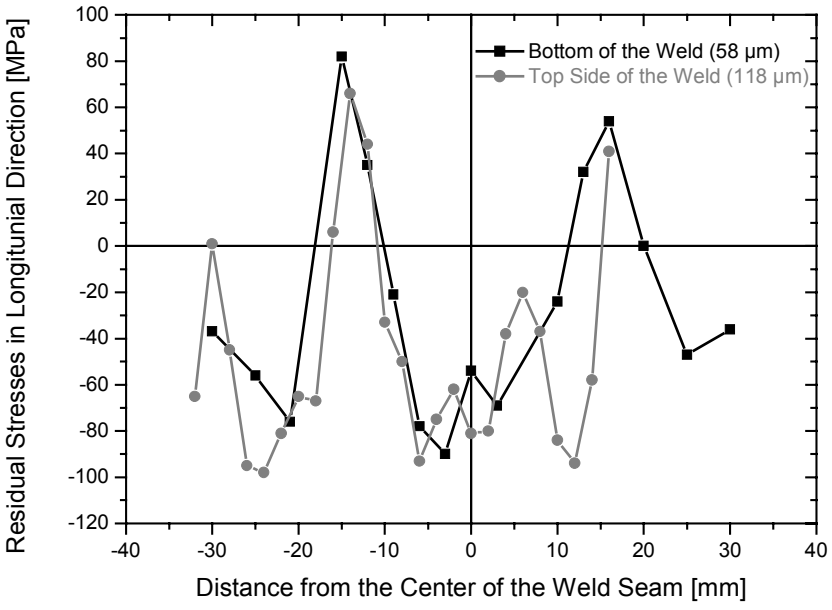

Figure 6: Comparison of the residual stress distribution at the top and root face of the friction stir weld. Sample welding parameters: tool rotational speed: 1500 min^{-1}; welding speed: 300 mm s^{-1}; tool diameter: 22 mm.

A comparison of the X-ray residual stress distribution obtained at the root face of the welds using with the residual stress distribution determined in 100µm distance from the root reveals only slight differences in the residual stress distribution. The residual stress values evaluated from the neutron diffraction measurements are however slightly lower in both the extreme values of the compressive as well as in the extreme value encountered for the tensile residual stresses. This is due to the averaging in the comparatively large gauge volumes necessary in case of neutron diffraction measurements. Peak values of residual stress are identified more precisely by using methods with higher local resolution such as measurements by X-ray and synchrotron radiation [16]. Details on the residual stress distribution across the weld thickness determined by using high energy synchrotron radiation will be given in a forthcoming paper.

A comparison of the residual stress values determined at the face and the bottom side of the welds shows that the residual stress distribution in the weld seam, in the thermo-mechanically affected zone and the heat affected zone is similar on both sides of the joint.

The influence of process parameters on the residual stress distribution is presented in Figure 7. The larger extension of the thermo-mechanically affected zones of the sheets joined with a larger shoulder increases the distance of the tensile stress peaks. The magnitude of the tensile residual stresses reached in the heat affected zone decreases with decreasing welding speed and decreasing rotational speed of the tool. This is caused by the decreasing heat produced with decreasing welding speed and tool rotational speed and the longer time interval available for the heat transfer into the parent material. The higher heat input and causes a widening of the heat affected zone and lower cooling rate results in a decrease of the magnitude of the residual stress values [17].

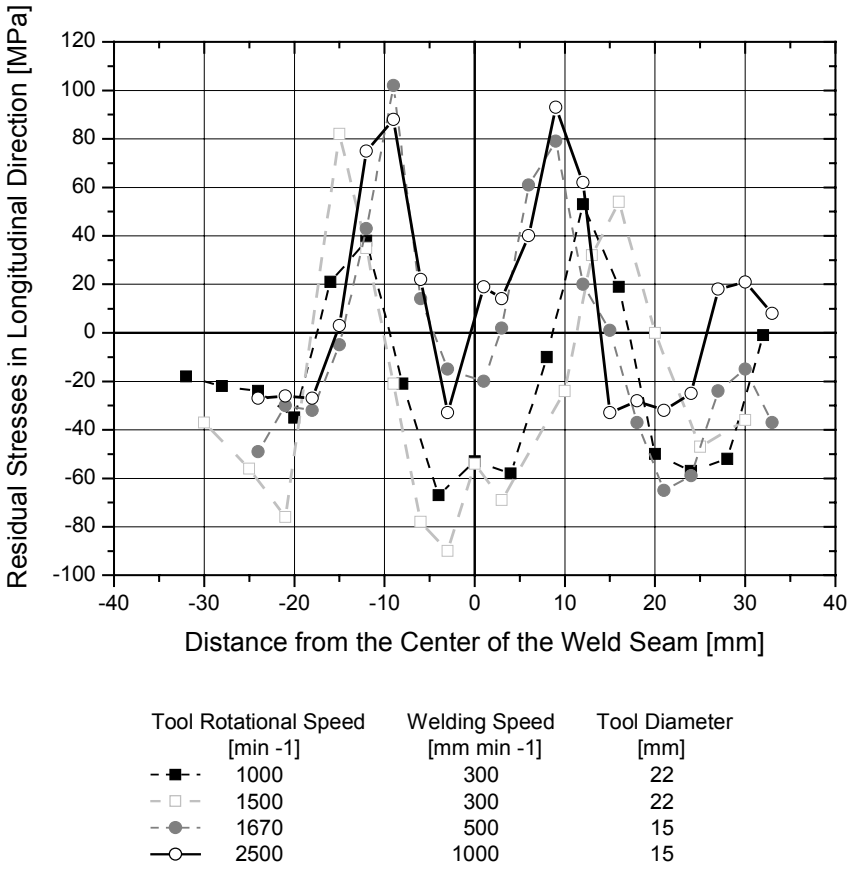

Figure 7: Residual stress distribution in dependence of the welding parameters. Measurements at the bottom side of the weld with X-Ray Cu-K_α radiation (Depth: 58 µm); Sample with 1000 min^{-1} tool rotation speed was measured with X-Ray Co-K_α radiation (Depth: 54 µm).

Summary and Conclusions

Residual stress analysis on friction stir welds were carried out by the cut compliance technique and by diffraction methods. The results of the experiments are in good quantitative and qualitative agreement. The longitudinal stresses are always higher than the transverse residual stresses and reveal an "M" like distribution with small compressive residual stresses in the weld seam and high tensile residual stresses in the heat affected zone. A comparison of the residual stress distributions obtained using X-rays, synchrotron X-rays and neutrons reveals that the peak values are only identified when a sufficiently high local resolution is used (such as X-rays for the root and top face of the weld and synchrotron radiation with a small gauge volume for the through-thickness measurements).

The influence of process parameters such as the tool size and the welding speed and the tool rotational speed were also investigated. The experiments show that larger tool diameters widen the M of the residual stress distribution. The magnitude of the tensile residual stresses reached in the heat affected zone decreases with decreasing welding speed and decreasing rotational speed of the tool.

From the investigation presented here and the known literature it seems that the peak tensile values of longitudinal residual stresses are in the range of 30 to 60 % of weld material yield strength and 20 % to 50 % of parent material yield strength if small samples like the ones used here are employed. Wang' s results [17] however indicate that larger stresses may be present in larger samples.

Acknowledgements

The authors wish to thank Mr. F. Palm from EADS Corporate Research Center, Munich, for kindly providing some of the FSW joints.

References

[1] Masubuchi, K.: *Analysis of Welded Structures*, Oxford, New York, Pergamon Press, 1980.

[2] Djapic Oosterkamp, L., Webster, P. J., Browne, P. A., Vaughan, G. B.M. and Withers, P.J.: Residual Stress Field in a Friction Stir Welded Aluminum Extrusion, *Metal Science Forum Vols. 347-349*, Trans Tech Publications, Switzerland, 2000, pp. 678-683.

[3] Jata, K.V., Sankaran, K.K and Ruschau, J. J.: Friction Stir Welding Effects on Microstructure and Fatigue of Aluminum Alloy 7050-T7451, *Metallurgical Transactions A*, 31A, 2000, pp. 2181-2192.

[4] Dalle Donne, C. and Raimbeaux, G.: Residual Stress Effects on Fatigue Crack Propagation in Friction Stir Welds, *10th International Conference on Fracture, ICF 10*, Elsevier Science Publ., 2001, pp. accepted for publication.

[5] Dalle Donne, C., Biallas, G., Ghidini, T. and Raimbeaux, G.: Effect of Weld Imperfections and Residual Stresses on the Fatigue Crack Propagation in Friction Stir Welded Joints, *Second International Conference on Friction Stir Welding*, 2000, cd-rom.

[6] Biallas, G., Braun, G., Dalle Donne, C., Staniek, G. and Kaysser, W.: Mechanical Properties and Corrosion Behavior of Friction Stir Welded 2024-T3, *1st International Symposium on Friction Stir Welding*, TWI, UK, 1999, pp. pdf-file.

[7] Braun, R., Biallas, G., Dalle Donne, C. and Staniek, G.: Characterisation of Mechanical Properties and Corrosion Performance of Friction Stir Welded AA6013 Sheet, *Materials*

for Transportation Technology EUROMAT '99 - Vol. 1, Winkler, P.J. (Ed.), Wiley-VCH, 1999, pp. 150-155.

[8] Schindler, H.-J., Cheng, W. and Finnie, I.: Experimental Determination of Stress Intesity Factors Due to Residual Stresses, *Experimental Mechanics*, 37, 3, 1997, pp. 272-277.

[9] Prime, M.B.: Residual Stress Measurement by Successive Extension of a Slot: The Crack Compliance Method, *Appl. Mech. Rev.*, 52, 1999, pp. 75-96.

[10] Fett, T. and Munz, D.: *Stress Intensity Factors and Weight Functions*, Southampton, UK, Computanional Mechanics Publications, 1997.

[11] Schindler, H.-J.: Determination of Residual Stress Distributions from Measured Stress Intensity Factors, *International Journal of Fracture*, 74, 1995, pp. R23-R30.

[12] Fett, T.: Stress Intensity Factors for Edge-Cracked Plates Under Arbitrary Loading, *Fatigue and Fracture of Engineering Materials and Structures*, 22, 1999, pp. 301-305.

[13] Prime, M.B.: Measuring Residual Stresses and the Resulting Stress Intensity Factor in Compact Tension Specimens, *Fatigue and Fracture of Engineering Materials and Structures*, 22, 1999, pp. 195-204.

[14] Reimers, W., Pyzalla, A., Broda, M., Brusch, G., Dantz, D., Liss, K.-D., Schmackers, T., Tschentscher, T.: The Use of High Energy Synchrotron Diffraction (HESD) for Residual Stress Analyses, *J. Mat. Sci. Letters*, 19, 1999, pp. 581 – 583

[15] Pyzalla, A.: Methods and feasibility of residual stress analysis by high energy synchrotron diffraction in transmission geometry using a white beam, *J. Nondestructive Evaluation,* 19, 2000, pp. 21 – 31

[16] Pyzalla, A.: Stress and strain measurements: X-rays and neutrons, *Physica B*, 276-278, 2000, pp. 833-836

[17] Wang, X.-L., Feng, Z., David, S., Spooner, S., Hubbard, C.S.: Neutron diffraction study of residual stresses in friction stir welds, *Proc. ICRS 6*, IOM Communications, London, UK (2000) 1408 – 1420